Lithography and reactive ion etching optimization towards low-loss TiO_2 waveguides

I. Hegeman, S.M. Garcia-Blanco
University of Twente, Optical Sciences, 7522NH Enschede, Netherlands

TiO_2 is emerging as material platform for integrated photonics [1–3]. *However, the propagation losses remain too high for industrial applications. In order to reduce the waveguide losses, effort is put on the optimization of the lithography and etching process. The sidewall roughness induced by etching is critical for the waveguide performance. To reduce sidewall roughness, negative E-beam lithography is used. A negative E-beam resist (ARN 7520.18) followed by the conductive coating (AR-PC 5091) are applied by spin-coating. An HMDS layer underneath the resist is utilized to improve adhesion to the substrate and therefore allow structures with high aspect ratio. Reactive ion etching with pure SF_6, CHF_3, HBr, Cl_2 and BCl_3 are compared. BCl_3 chemistry showed to be most beneficial. The influence of additional Ar and O_2 flow and varying the HF power and pressure to etching in BCl_3 are reported.*

Introduction

TiO_2 is an emerging material for integrated photonics [1–3]. The high refractive index of around 2.3 allows to scale down integrated photonic circuits and the bandgap of higher than 3 eV [4] results in a large transparency window. Because of the high non-linearity, four-wave mixing [2], supercontinuum generation [3] and third harmonic generation [5] have been demonstrated. Furthermore the negative thermo-optic coefficient [6] (TOC) can be used to design athermal devices by combining TiO_2 with a material with a positive TOC such as Si_3N_4 [7] or Si [8]. The optical propagation losses remain however relatively high and go down to 9.7 dB/cm at a wavelength of 633 nm [9] and 4 dB/cm at 1550 nm [10], when using conventional fabrication techniques, i.e. deposition, lithography and etching. By using a lift-off process, lower losses of 7.5 and 1.2 dB/cm at 633 nm and 1550 nm respectively can be obtained [1].

In most cases, etching of TiO_2 is performed using reactive ion etching (RIE) with fluorine as chemical component [2,9–11], often with addition of O_2 and Ar. These processes are however all performed by using a Cr or Al hard mask, made by E-beam lithography (EBL) using positive resist, followed by lift-off. Using only negative resist would result in a much simpler process.

Several studies have been performed to compare the RIE characteristics of TiO_2 in different chemicals. These studies include etching with SF_6, CH_3 and Cl_2 [12], HBr and Cl_2 mixtures [13], $CF_4/Ar/N_2$ [14], $CF_4/Ar/O_2$ [15], SF_6/Ar, CF_4/O_2 and CF_4/Ar [16] and BCl_3/Ar [17]. These studies however do not show the selectivity of TiO_2 towards resist, which is a crucial factor for waveguide fabrication. Furthermore, many studies are performed by different groups, which makes it hard to compare different chemistries quantitatively.

In this work, we show the development of a process recipe for negative EBL resist. The etch rates of the EBL resist, SiO_2 and TiO_2 are compared for different RIE chemistries. For BCl_3 the influence of assisting gasses and different etching parameters are compared to optimize the etching recipe.

E-beam lithography

For the EBL process a negative resist (ARN 7520.18) is spin coated on top of a 4 inch Si wafer with an 8 μm thermal oxide layer. The spin coating is performed for 3 minutes at 1500 rpm, followed by a baking step of 1 minute at 85 °C. The E-beam exposure is performed using the Raith EBPG5150 with an accelaration voltage of 100 kV. Comparing the structures written with

different doses, showed an optimum dose of 1000 μC/cm^2. After exposure, the patterns are developed in undiluted AR 300-47 developer for 1 minute. The resist patterns contain lines with a width varying between 300 and 1000 nm and gaps between 100 and 1000 nm. The resist showed bad adhesion to the substrate, causing the resist patterns to release or stick together. An example is shown in figure 1(a). The electrically insulating substrate causes charge build up during the exposure. As a result, stitching errors occur between write fields, causing shifts of up to several micrometers in the patterns, shown in figure 1(b).

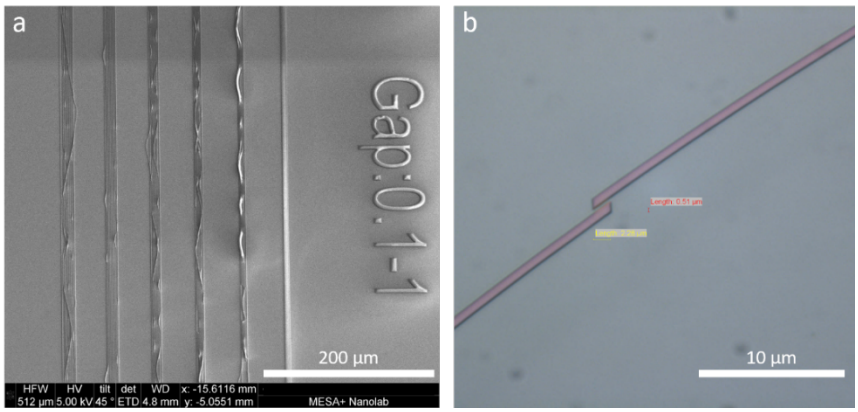

Fig. 1. (a) SEM of negative E-beam resist lines showing bad adhesion to the substrate. (b) Microscope image showing typical stitching errors between write fields during E-beam lithography, as a result of charging of the substrate.

To improve the adhesion of the resist to the substrate, an HMDS layer is spin coated for 45 seconds at 4000 rpm, prior to the spin coating of the resist. In order to prevent charge build up, a conductive coating (AR-PC 5091) is applied on top of the resist. This is also performed by spin coating for 45 seconds at 2000 rpm. The resulting patterns are shown in figure 2. The height of the resist is around 670 nm, with small variations per process. Stitching errors do not occur and good adhesion of the resist to the substrate is obtained. Patterns show to be 50 nm narrower than designed, causing gap sizes to be 50 nm wider. As shown in figure 2b, gaps of 150 nm are well defined and opened during development. Smaller gaps might be possible, but these are not tested, since 150 nm is sufficient for waveguide design.

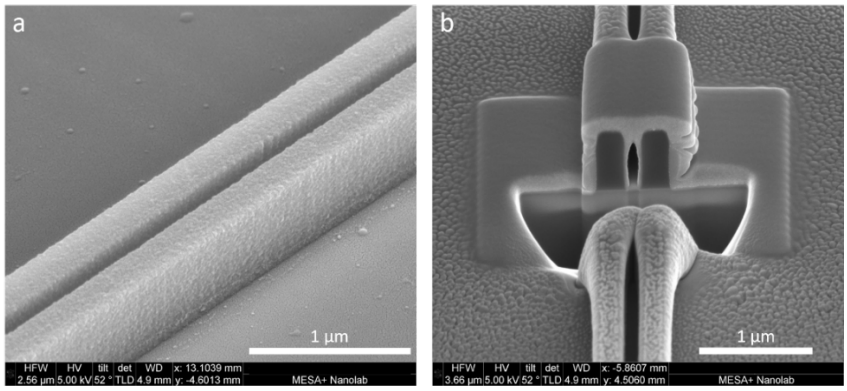

Fig. 2. SEM image of 650 nm thick and 250 nm wide negative E-beam resist lines with a gap of 150 nm on top of a SiO_2 substrate, (a) sideview (b) cross section.

Etching

The RIE is performed using the Oxford Plasma Pro 100 Cobra. The relevant etch parameters are shown in table 1. In each case, 25 sccm is used for the reactive gas flow. The etch rates in the 5 different available chemistries are compared and summarized in table 2. Etch rates of TiO_2 are measured by ellipsometry before and after etching using the Woollam M-2000UI. Etch rates

of the negative resist and SiO_2 are measured by measuring the step height before etching, after etching and after stripping the resist. This is done with the Veeco Dektak 8.

Pressure (mTorr)	Time (mm:ss)	HF power (W)	ICP power (W)	Temperature (°C)
10	01:00	20	1500	10

Table 1. Etch parameters

	SF_6	CHF_3	HBr	Cl_2	BCl_3
Resist	175	36	20	77	34
SiO_2	71	73	10	~0*	15
TiO_2	55	15	~0*	4	45

Table 2. Etch rates for different reactive gasses with a flow of 25 sccm
*no etching measured within measurement limit

RIE with BCl_3 shows the second highest etching speed of TiO_2, and the best selectivity of 1.29 towards resist and 3 towards SiO_2. The characteristics of BCl_3 etching are determined as a function of Ar and O_2 flow, HF Power and pressure. The etching rates are shown in figure 3. The BCl_3 flow is kept at 25 sccm and the other parameters are given in table 1, except for figure 3(c-d) where the HF power and pressure are increased.

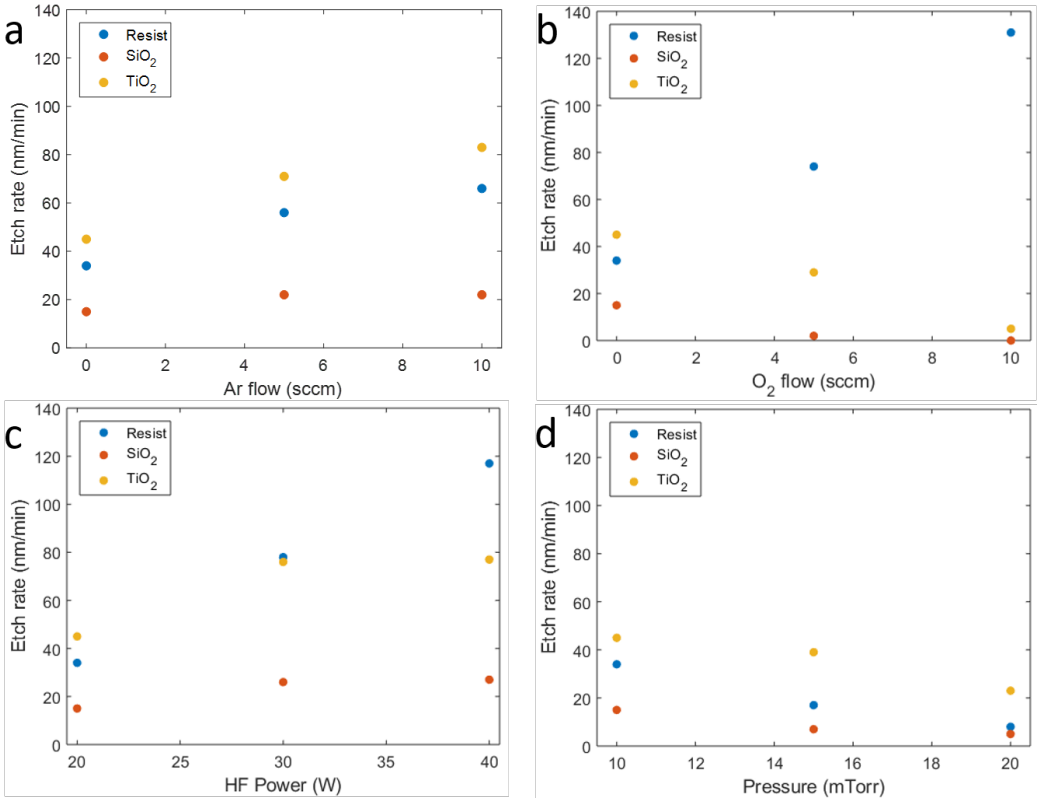

Figure 3. Etching rates of the negative E-beam resist, SiO_2 and TiO_2 for varying (a) Ar flow, (b) O_2 flow, (c) HF power and (d) pressure.

As shown in figure 3(a), the etching speed of TiO_2 and resist increase, but the selectivity stays the same. By adding some Ar into the plasma, the physical etching component increases, which increases the etching rate. Figure 3(b) shows that adding O_2 into the chamber decreases the SiO_2 and TiO_2 etching rate and increases the etching rate of the resist, resulting in very low selectivity of TiO_2 towards resist of 0.04 for 10 sccm of O_2. Applying a higher HF power increases the etching speeds, but the selectivity reduces as shown in figure 3(c). Finally the

pressure is increased, which results in lower etching rates, caused by the decreased acceleration of the ions due to the increased number of ions. However the selectivity of TiO_2 towards resist goes up to 2.9.

Conclusion

An EBL process has been developed to get resist patterns down to a width of 250 nm with a gap down to 150 nm by using negative E-beam resist. Stitching errors are prevented by applying a conductive coating and the adhesion to the substrate is improved with an interstitial HMDS layer. Etching with BCl_3 showed to be most beneficial for etching TiO_2, compared to SF_6, CHF_3, Cl_2 and HBr. Selectivities towards the negative resist of 2.9 are obtained. Further optimization of the etching parameters might increase the selectivity.

Funding

This work is part of the research programme Industrial Doctorates with project number NWA.ID.17.100, which is financed by the Dutch Research Council (NWO).

References

1. C. C. Evans, C. Liu, and J. Suntivich, "Low-loss titanium dioxide waveguides and resonators using a dielectric lift-off fabrication process," Opt. Express **23**, 11160–1169 (2015).
2. X. Guan, H. Hu, L. K. Oxenløwe, and L. H. Frandsen, "Compact titanium dioxide waveguides with high nonlinearity at telecommunication wavelengths," Opt. Express **26**, 1055–1063 (2018).
3. K. Hammani, L. Markey, M. Lamy, B. Kibler, J. Arocas, J. Fatome, A. Dereux, J.-C. Weeber, and C. Finot, "Octave Spanning Supercontinuum in Titanium Dioxide Waveguides," Appl. Sci. **8**, 543 (2018).
4. M. Landmann, E. Rauls, and W. G. Schmidt, "The electronic structure and optical response of rutile, anatase and brookite TiO_2," J. Phys. Condens. Matter **24**, 195503 (2012).
5. C. C. Evans, K. Shtyrkova, O. Reshef, M. Moebius, J. D. B. Bradley, S. Griesse-Nascimento, E. Ippen, and E. Mazur, "Multimode phase-matched third-harmonic generation in sub-micrometer-wide anatase TiO_2 waveguides," Opt. Express **23**, 7832–7841 (2015).
6. O. Reshef, K. Shtyrkova, M. G. Moebius, S. Griesse-Nascimento, S. Spector, C. C. Evans, E. Ippen, and E. Mazur, "Polycrystalline anatase titanium dioxide microring resonators with negative thermo-optic coefficient," J. Opt. Soc. Am. B **32**, 2288–2293 (2015).
7. F. Qiu, A. M. Spring, and S. Yokoyama, "Athermal and high-Q hybrid TiO_2-Si_3N_4 ring resonator via an etching-free fabrication technique," ACS Photonics **2**, 405–409 (2015).
8. B. Guha, J. Cardenas, and M. Lipson, "Athermal silicon microring resonators with titanium oxide cladding," Opt. Express **21**, 26557–26563 (2013).
9. M. Furuhashi, M. Fujiwara, T. Ohshiro, M. Tsutsui, K. Matsubara, M. Taniguchi, S. Takeuchi, and T. Kawai, "Development of microfabricated TiO_2 channel waveguides," AIP Adv. **1**, 032102 (2011).
10. J. D. B. Bradley, C. C. Evans, J. T. Choy, O. Reshef, P. B. Deotare, F. Parsy, K. C. Phillips, M. Lončar, and E. Mazur, "Submicrometer-wide amorphous and polycrystalline anatase TiO_2 waveguides for microphotonic devices," Opt. Express **20**, 23821–23831 (2012).
11. M. Häyrinen, M. Roussey, A. Säynätjoki, V. Gandhi, L. Karvonen, P. Stenberg, M. Kuittinen, and S. Honkanen, "Low-loss titanium-dioxide strip waveguides by atomic layer deposition," SPIE Photonics West 2014-OPTO Optoelectron. Devices Matter. **8982**, 89820E (2014).
12. S. Norasetthekul, P. Y. Park, K. H. Baik, K. P. Lee, J. H. Shin, B. S. Jeong, V. Shishodia, E. S. Lambers, D. P. Norton, and S. J. Pearton, "Dry etch chemistries for TiO_2 thin films," Appl. Surf. Sci. **185**, 27–33 (2001).
13. D. Kim, A. Efremov, H. Jang, S. Kang, S. J. Yun, and K.-H. Kwon, "Etching characteristics and mechanisms of TiO_2 thin films in $HBr/Cl_2/Ar$ inductively coupled plasma," Jpn. J. Appl. Phys. **51**, (2012).
14. K. R. Choi, J. C. Woo, Y. H. Joo, Y. S. Chun, and C. Il Kim, "The dry etching characteristics of TiO_2 thin films in $N_2/CF_4/Ar$ plasma," Trans. Electr. Electron. Mater. **15**, 32–36 (2014).
15. I. Hotovy, S. Hascik, M. Gregor, V. Rehacek, M. Predanocy, and A. Plecenik, "Dry etching characteristics of TiO_2 thin films using inductively coupled plasma for gas sensing," Vacuum **107**, 20–22 (2014).
16. R. Adzhri, M. K. M. Arshad, M. F. M. Fathil, U. Hashim, A. R. Ruslinda, R. M. Ayub, S. C. B. Gopinath, C. H. Voon, K. L. Foo, M. N. M. Nuzaihan, A. H. Azman, and M. Zaki, "Reactive Ion etching of TiO_2 thin film: The impact of different gaseous," RSM 2015 - 2015 IEEE Reg. Symp. Micro Nano Electron. Proc. 1–4 (2015).
17. J. C. Woo, Y. S. Chun, Y. H. Joo, and C. I. Kim, "The dry etching property of TiO_2 thin films using metal-insulator-metal capacitor in inductively coupled plasma system," Vacuum **86**, 2152–2157 (2012).